J Intell Robot Syst (2016) 84:163–177
DOI 10.1007/s10846-015-0295-y

LPV Model-Based Tracking Control and Robust Sensor Fault Diagnosis for a Quadrotor UAV

Francisco Ronay López-Estrada · Jean-Christophe Ponsart · Didier Theilliol · Youmin Zhang · Carlos-Manuel Astorga-Zaragoza

Received: 14 December 2014 / Accepted: 15 October 2015 / Published online: 6 November 2015

Abstract This work is dedicated to the design of a robust fault detection and tracking controller system for a UAV subject to external disturbances. First, a quadrotor modelled as a Linear Parameter Varying (LPV) system is considered as a target to design and to illustrate the proposed methodologies. In order to perform fault detection and isolation, a robust LPV observer is designed. Sufficient conditions to guarantee asymptotic stability and robustness against disturbance are given by a set of feasible Linear Matrix Inequalities (LMIs). Furthermore, the observer gains are designed with a desired dynamic by considering pole placement based on LMI regions. Then, a fault detection and isolation scheme is considered by mean of an observer bank in order to detect and isolate sensor faults. Second, a feedback controller is designed by considering a comparator integrator control scheme. The goal is to design a robust controller, such that the UAV tracks some reference positions. Finally, some simulations in fault-free and faulty operations are considered on the quadrotor system.

Keywords Quadrotor · LPV systems · LPV observer · Fault diagnosis · Tracking controller · Sensor fault

F. R. López-Estrada
Tecnológico Nacional de México, Instituto Tecnológico de Tuxtla Gutiérrez, Electronic Department, Carretera Panamericana km 1080, Terán, CP 29050, Tuxtla Gutiérrez, Chiapas, Mexico
e-mail: frlopez@ittg.edu.mx

J.-C. Ponsart (✉) · D. Theilliol
University of Lorraine, CRAN, CNRS UMR 7039, Campus Sciences, B.P. 70239, 54506 Vandoeuvre-les-Nancy Cedex, France
e-mail: Jean-Christophe.Ponsart@univ-lorraine.fr

D. Theilliol
e-mail: Didier.Theilliol@univ-lorraine.fr

Y. M. Zhang
Concordia University, 1455 de Maisonneuve Blvd. W., Montreal, Quebec H3G 1M8, Canada
e-mail: youmin.zhang@concordia.ca

C. M. Astorga-Zaragoza
Tecnológico Nacional de México, Centro Nacional de Investigación y Desarrollo Tecnológico (CENIDET), Internado Palmira s/n, Col. Palmira, CP 62490, Cuernavaca, Mor., Mexico
e-mail: astorga@cenidet.edu.mx

1 Introduction

In the recent years, quadrotor helicopter has become a popular Unmanned Aerial Vehicle (UAV) [14]. Quadrotor UAVs have been proved to be effective mobile platforms in the tasks such as surveillance, search, rescue, remote sensing, geographic studies, recognition, aerial transportation, inspection and maintenance, among others [32]. Comparing to a conventional helicopter, a quadrotor is essentially simpler to build. Nonetheless, the differential equations describing the dynamics of the quadrotor are high nonlinear, unstable and constantly affected by aerodynamic disturbances [22].

An attractive alternative to represent nonlinear dynamics is through Linear Parameter Varying (LPV) system approach. LPV systems are mathematical models that are able to exactly represent or to approximate a large class of nonlinear systems with an arbitrary degree of accuracy in a compact set of Linear Time Invariant (LTI) models [28]. Convex gain scheduling functions are considered to interpolate the local models, and then obtain a global representation of the nonlinear system. Note that in the past, the gain scheduling functions were computed by considering Takagi-Sugeno (T-S) fuzzy rules as defined in [29]. Nevertheless, T-S and polytopic LPV systems are described by the same form. Then, the community of researchers working on TS models uses the name "TS fuzzy systems", even if with the recent modeling approaches (for example sector nonlinearity transformation), the obtained model is no "fuzzy" because the weighting functions are completely deterministic that corresponds to LPV or quasi-LPV (qLPV) systems as detailed in [23].

The main advantage of qLPV systems is the capability of representing exactly a nonlinear model, which is affine in the control, in a compact set of the state variables [31]. Moreover, it is possible to apply control techniques developed for linear systems such as Linear Matrix Inequality (LMI), optimization methods, among others. Furthermore, LPV theory can be combined with H_2, H_-, and H_∞ as shown in [16], to produce enhanced control laws with performance and robustness specifications [2]. In the literature, there are many works for LPV systems involving different topics as observer design [5], feedback control [1], and fault diagnosis [17, 30]. LPV models of quadrotors have been proposed with good results on observer design [13], stabilization [12], and control [27].

Beyond the difficulties of the control systems design, there is also the demand of reliability and safety to maintain stability and an acceptable system performance in the presence of component and/or instrument faults [3, 26], which may cause the crash of the UAV. As reported by the Office of the Secretary of Defence of USA, development of self-repairing, smart flight control systems is a crucial step in the overall advancement of UAV autonomy [20]. To deal with this problem, Fault Diagnosis (FD) techniques are proposed to identify malfunctions at any time during flight. In FD, the generation of residual signals is the core element of diagnosis. There are many ways to generate residuals by observer design, parity space, adaptive observers, among others. More detailed information can be consulted in survey papers [25, 33]. Some applications of LPV control theory and FD to UAVs can be found in [10, 21, 24]. It is worth highlighting that only few works are reported that consider FD and LPV techniques applied to UAVs. Moreover, the aim of this paper is not only to consider LPV and FD, but also to apply a tracking LPV controller, which has not been treated so far.

The main contribution of this paper is to develop a robust fault diagnosis residual generator and tracking controller for a quadrotor system modelled as LPV system. The results presented in this work are an extension of our previous work in [18], with a significant extension by considering disturbance rejection, robust pole placement, and robust tracking controller. The observer and controller are designed based on Lyapunov and $\mathscr{L}_2$-gain theory in order to minimize the effect of disturbances. In addition, the tracking controller is designed by considering an integrator-comparator block and the LPV system. A bank of residual generators based on Generalized Observer Scheme (GOS) is built to perform robust fault detection and isolation. Finally, the fault diagnosis and the tracking controller are applied to the quadrotor to illustrate the proposed method.

The paper is organized as follows. In Section 2, the dynamic model of the quadrotor and a general formulation of the problem are given. Section 3 is dedicated to the presentation of the main results: the observer design is developed in first, then the sensor fault detection and isolation is considered and finally the tracking-controller is designed. Section 4 represents the simulation results in order to show the effectiveness of the methodology when it is applied to the quadrotor. Concluding remarks are given at the end.

Notations The notations used in this article are standard. For a matrix $A \in \mathbb{R}^{m\times n}$, A^T, A^{-1} and $A^\dagger$ denote its transpose, inverse and pseudoinverse respectively. The symbol $*$ denotes the transposed element in the symmetric positions of a matrix. He$\{A\}$ is a shorthand notation for $A + A^T$.

2 Dynamic Model and Problem Definition

The quadrotor is a helicopter composed of four inputs provided by each propeller and six outputs as shown in Fig. 1. The system under consideration is the nonlinear model adopted from [19, 27], and the LPV system given in [12]. From the parameters shown in Table 1, the states and the control inputs of a quadrotor UAV are defined as:

$$x = \left[x_{0,}\, y_0,\, z_0,\, \psi,\, \theta,\, \phi,\, u_{0,}\, v_{0,}\, \omega_0,\, p,\, q,\, r_o\right]^T \quad (1)$$

$$u = \left[\, u_1 \; u_2 \; u_3 \; u_4 \,\right]^T, \quad (2)$$

The nonlinear model for the quadrotor is given by the following equations

$$\dot{x} = f(x) + \sum_{i=1}^{4} g_i(x) u_i \quad (3)$$

where

$$f(x) = \begin{bmatrix} u_0 \\ v_0 \\ \omega_0 \\ q \sin\phi \sec\theta + r_o \cos\phi \sec\theta \\ q\cos\phi - r_o \sin\phi \\ p + q \sin\phi \tan\theta + r_o \cos\phi \tan\theta \\ \frac{A_x}{m} \\ \frac{A_y}{m} \\ \frac{A_z}{m} + g \\ \frac{I_y - I_z}{I_x} q r_o + \frac{A_p}{I_x} \\ \frac{I_z - I_x}{I_y} p r_o + \frac{A_p}{I_y} \\ \frac{I_x - I_y}{I_z} q r_o + \frac{A_r}{I_z} \end{bmatrix}$$

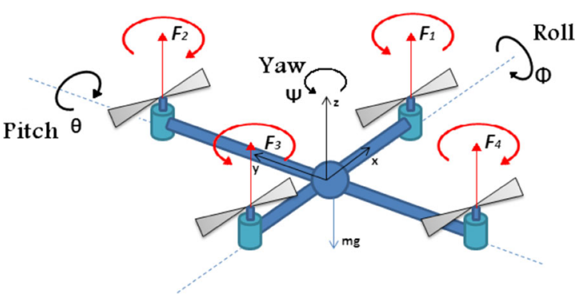

Fig. 1 Quadrotor configuration

and,

$$g_1(x) = \left[0,\, 0,\, 0,\, 0,\, 0,\, 0,\, g_{1,7},\, g_{1,8},\, g_{1,9},\, 0,\, 0,\, 0\right]^T$$

$$g_2(x) = \left[0,\, 0,\, 0,\, 0,\, 0,\, 0,\, 0,\, 0,\, 0,\, \frac{d}{I_x},\, 0,\, 0\right]^T$$

$$g_3(x) = \left[0,\, 0,\, 0,\, 0,\, 0,\, 0,\, 0,\, 0,\, 0,\, 0,\, \frac{d}{I_y},\, 0\right]^T$$

$$g_4(x) = \left[0,\, 0,\, 0,\, 0,\, 0,\, 0,\, 0,\, 0,\, 0,\, 0,\, 0,\, \frac{I}{I_z}\right]^T,$$

with

$$g_{1,7} = -\frac{1}{m}\left(\cos\phi \cos\psi \sin\theta + \sin\phi \sin\psi\right)$$

$$g_{1,8} = -\frac{1}{m}\left(\cos\phi \sin\theta \sin\psi - \cos\psi \sin\phi\right)$$

$$g_{1,9} = -\frac{1}{m}\left(\cos\theta \cos\phi\right).$$

To obtain the LPV equations of the quadrotor, the nonlinear model is linearized around different operation points. Then, by considering the different sub-models the following representation is obtained

$$\dot{x}(t) = \sum_{i=1}^{h} \rho_i(x(t)) \left[A_i x(t) + B_i u(t) + R_i d(t)\right]$$

$$y(t) = C x(t) + D_d d(t) \quad (4)$$

where $x(t) \in \mathbb{R}^n$, $u(t) \in \mathbb{R}^m$, $d(t) \in \mathbb{R}^q$, and $y(t) \in \mathbb{R}^p$ are the state vector, the control input, the disturbance, and the measured output vector respectively. A_i, B_i, R_i, C, and D_d are constant matrices of appropriate dimensions. $\rho_i(x(t))$ are scheduling functions which depend on $x(t)$. The scheduling functions of the h sub-models satisfy the following convex set sum property:

$$\forall i \in [1, 2, ..., h],\; \rho_i(x(t)) \geq 0,\; \sum_{i=1}^{h} \rho_i(x(t)) = 1, \forall t. \quad (5)$$

By assuming observable outputs and to generate the residuals, a robust fault diagnosis observer of Eq. 4 described by the following equations is considered

$$\dot{z}(t) = \sum_{i=1}^{h} \rho_i(x(t)) \left[N_i z(t) + G_i u(t) + L_i y(t)\right] \quad (6)$$

$$\hat{x}(t) = z(t) + T_2 y(t)$$

$$r(t) = W(y(t) - C\hat{x}(t)), \quad (7)$$

Table 1 Variables and parameters of the quadrotor UAV

Parameter (unit)	Symbol	Value
Position (m)	(x_o, y_o, z_o)	–
Velocity (m/s)	(u_0, v_0, ω_0)	–
Angular velocity expressed in a body reference frame (rad/s)	(p, q, r_o)	
Euler angles yaw, pitch and roll (rad)	(ψ, θ, ϕ)	–
Resulting thrust of the four rotors	u_1	–
Difference of thrust between the left rotor and the right rotor	u_2	–
Difference of thrust between the front rotor and the back rotor	u_3	–
Difference of torque between the two clockwise turning rotors and the two counter-clockwise turning rotors	u_4	–
Mass (kg)	m	0.7
Aerodynamic forces and moments acting on the UAV.	$(A_x, A_y, A_z)^T$ and $(A_p, A_q, A_r)^T$	–
Moments of inertia along the x, y, and z directions ($kg \cdot m^2$)	$\begin{bmatrix} I_x \\ I_y \\ I_z \end{bmatrix}$	$\begin{bmatrix} 1.241 \\ 1.241 \\ 1.241 \end{bmatrix}$
Gravity of earth (m/s^2)	g	9.81
Distance from the motors to the centre of gravity (m)	d	0.3

where $z(t)$ represents the state vector of the observer, $\hat{x}(t)$ the estimated state vector. N_i, G_i, L_i, and T_2 are the gain matrices of Eq. 6 to be synthesized. $r(t)$ is the residual signal and W the residual weighting matrix to determine. The gain matrices of the fault diagnosis observer (6) must be designed in order to guarantee the convergence of the state estimation error and maximize the robustness against disturbances $d(t)$.

The second objective is to design a feedback controller such that the steady-state response tends to $\lim_{t\to\infty} y(t) := w(t)$, where $w(t)$ is the desired position. To reach the desired position an integrator comparator is added as shown in Fig. 2, such that

$$\dot{\epsilon}(t) = w(t) - y(t) = w(t) - Cx(t) - D_d d(t). \quad (8)$$

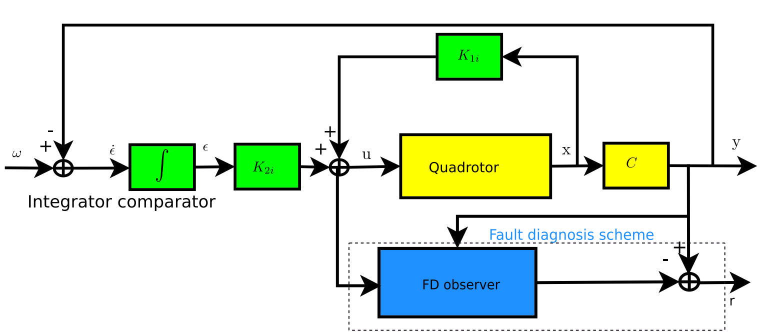

Fig. 2 Fault diagnosis and tracking controller scheme

The control law $u(t)$ is given by the following feedback controller

$$u(t) = K_{1i}x(t) + K_{2i}\epsilon(t) = \mathcal{K}_i \begin{bmatrix} x(t) \\ \epsilon(t) \end{bmatrix}, \tag{9}$$

where K_{1i} and K_{2i} are the state feedback gains matrices to be synthesised. Then, the problem is reduced to determine optimal values of the controller gains.

3 Main Result

3.1 Observer Design

The estimation error is defined as

$$e(t) = x(t) - \hat{x}(t) \tag{10}$$
$$e(t) = (I - T_2C)x(t) - z(t) - T_2D_dd(t), \tag{11}$$

Under the assumption $T_1 \in \mathbb{R}^{n\times n}$ matrix such that

$$T_1 = I - T_2C \tag{12}$$

In order to eliminate $d_d(t)$ from Eq. 11, the following condition is considered

$$T_2D_d = 0 \tag{13}$$

Then, by considering Eqs. 12–13, the dynamic of the error equation is computed as

$$\begin{aligned}
\dot{e}(t) &= T_1\dot{x}(t) - \dot{z}(t) \\
\dot{e}(t) &= \sum_{i=1}^{h} \rho_i(x(t)) [T_1A_ix(t) + T_1B_iu(t) + T_1R_id(t) \\
&\quad -N_iz(t) - G_iu(t) - L_i(Cx(t) + D_dd(t))] \qquad (14) \\
\dot{e}(t) &= \sum_{i=1}^{h} \rho_i(x(t)) [(T_1A_i - L_iC - N_iT_1)x(t) + (T_1B_i - G_i)u(t) \\
&\quad + (T_1R_i - L_iD_d)d(t) + N_ie(t)] \qquad (15)
\end{aligned}$$

Let us consider also the following equations:

$$0 = T_1A_i - L_iC - N_iT_1 \tag{16}$$
$$G_i = T_1B_i \tag{17}$$

By considering the error equation (11), the assumptions Eqs. 12, and 16, the following gain synthesis is obtained

$$N_i = T_1A_i - K_iC \tag{18}$$
$$K_i = L_j - N_iT_2. \tag{19}$$

A particular solution of matrices T_1 and T_2 is computed as:

$$\begin{bmatrix} T_1 & T_2 \end{bmatrix} = \begin{bmatrix} I_n & 0 \end{bmatrix} \begin{bmatrix} I & 0 \\ C & D_d \end{bmatrix}^{\dagger}. \tag{20}$$

Then, under previous gain synthesis and by considering the residual equation (7), the residual state-space error system is given by

$$\mathcal{G}_e := \begin{cases} \dot{e}(t) = \sum_{i=1}^{h} \rho_i(x(t) [N_ie(t) + (T_1R_i - K_iD_d)d(t)] \\ r(t) = WCe(t) + WD_dd(t). \end{cases}$$

Then, the problem is reformulated in order to guarantee asymptotic stability of the error system $\mathcal{G}_e$ despite the disturbance vector $d(t)$. The following Theorem gives sufficient conditions to achieve this objective.

Theorem 1 *Consider the system (4) and the observer (6), and let the attenuation level, $\gamma > 0$. The quadratic stability of the estimation error is guaranteed if $\| \mathcal{G}_e \|_\infty < \gamma$ and if there exist matrices $P = P^T > 0$, Q_j and Φ_i, such that the following holds $\forall i, j \in [1, 2, ..., h]$:*

$$\begin{bmatrix} \mathrm{He}\left(A_i^TQ - C^T\Phi_i^T\right) & PT_1R_i - \Phi_iD_d & (WC)^T \\ * & -\gamma^2 I & (WD_d)^T \\ * & * & -I \end{bmatrix} < 0 \tag{21}$$

where T_1 is given by

$$\begin{bmatrix} T_1 & T_2 \end{bmatrix} = \begin{bmatrix} I_n & 0 \end{bmatrix} \begin{bmatrix} I & 0 \\ C & D_d \end{bmatrix}^{\dagger}.$$

Then, the observer parameters are computed by $K_i = P^{-1}\Phi_i$ and the relation given in Eqs. 18–17.

Proof In order to guarantee asymptotic convergence to zero of the estimation error and robustness against disturbances $d(t)$, the following H_∞ criterion is considered

$$J_{rd} := \dot{\Omega}(t) + J_1 < 0 \tag{22}$$

$$J_1 := r^T(t)r(t) - \gamma^2 d^T(t)d(t) < 0, \tag{23}$$

where J_{rd} represents the $\mathcal{L}_2$ gain of system (21) (from $d(t)$ to $r(t)$) bounded by γ. $\Omega(t)$ is a Lyapunov function defined as $\Omega(t) = V(x_e(t)) = e^T(t)Pe(t)$.

The derivate of the Lyapunov function is synthesized as:

$$\dot{\Omega}(t) = \dot{e}^T(t)Pe(t) + e^T(t)P\dot{e}(t) \tag{24}$$

Then, by considering Eq. 21, the following is equivalent

$$\begin{aligned}\dot{\Omega}(t) &= (N_i e(t) + (T_1 R_i - K_i D_d)\, d(t))^T \, Pe(t) \\ &\quad + e^T(t)P\,(N_i e(t) \, + (T_1 R_i - K_i D_d)) \end{aligned} \tag{25}$$

$$\dot{\Omega}(t) = \begin{bmatrix} e(t)^T \\ d(t)^T \end{bmatrix}^T \begin{bmatrix} N_i^T P + PN_i & PT_1 R_i - PK_i D_d \\ * & 0 \end{bmatrix} \times \begin{bmatrix} e(t) \\ d(t) \end{bmatrix}. \tag{26}$$

By manipulating Eq. 23, the following is obtained

$$J_1 := \begin{bmatrix} C^T W^T WC & 0 \\ * & -\gamma^2 I \end{bmatrix}. \tag{27}$$

Then, by considering Eqs. 26 and 27, the condition (22) is rewritten as

$$\begin{bmatrix} e(t)^T \\ d(t)^T \end{bmatrix}^T \Lambda_i \begin{bmatrix} e(t) \\ d(t) \end{bmatrix} < 0, \tag{28}$$

where

$$\Lambda_i = \begin{bmatrix} N_i^T P + PN_i + C^T W^T WC & PT_1 R_i - PK_i D_d \\ * & -\gamma^2 I \end{bmatrix}. \tag{29}$$

Then by considering N_i from Eq. 18, and defining $\Phi_i = PK_i$ in order to eliminate the quadratic term, Λ_i is manipulated as:

$$\Lambda_i = \begin{bmatrix} \mathrm{He}\left(A_i^T Q - C^T \Phi_i^T\right) + C^T W^T WC & PT_1 R_i - \Phi_i D_d \\ * & -\gamma^2 I \end{bmatrix}. \tag{30}$$

Hence, if $\Lambda_i < 0$ implies $J_{rd} < 0$. Finally the Schur complement implies (21). This ends the proof. □

Theorem 1 guarantee an asymptotic stability of the estimation error (21). Nevertheless in order to improve the observer performance, the observer gains can be placed in a defined LMI region $\mathcal{D}$. The definition of the LMI region is given as:

Definition 1 (LMI region [7]) The subset $\mathcal{D}$ of the complex left half plane is called LMI region if there exist a matrix $\alpha \in \mathbb{R}^{n\times n}$ and matrix $\beta \in \mathbb{R}^{n\times n}$ such as

$$\mathcal{D} = \left\{ z \in \mathcal{C} : f_D(z) = \alpha + z\beta + \bar{z}\beta^T < 0 \right\} \tag{31}$$

Then by considering Definition 1, it is possible to locate the observer gains in the domain of $\mathcal{D}$ of the complex-left half plane. Then by considering the method given in [7], the following corollary of Theorem 1 is obtained:

Corollary 1 *Consider the system* (4) *and the observer* (6)*, and let the attenuation level,* $\gamma > 0$. *The quadratic stability of the estimation error is guaranteed if* $\| \mathcal{G}_e \|_\infty < \gamma$ *and if there exist matrices* $P = P^T > 0$, Q_j *and* Φ_i*, such that the eigenvalues are assignment in a disk* $\mathcal{D}(\varrho, \delta)$ *with center*$(-\varrho, 0)$ *and radius* δ*, and the following holds* $\forall i, j \in [1, 2, ..., h]$*:*

$$\left[\begin{array}{cc|c|c} -\delta P & \varrho P + A_i^T Q - C^T \Phi_i^T & PT_1 R_i - \Phi_i D_d & 0 \\ * & -\delta P & 0 & C^T W^T \\ * & * & -\gamma^2 I & D^T W^T \\ * & * & * & -I \end{array}\right] < 0 \tag{32}$$

where T_1 *is given by*

$$\begin{bmatrix} T_1 & T_2 \end{bmatrix} = \begin{bmatrix} I_n & 0 \end{bmatrix} \begin{bmatrix} I & 0 \\ C & D_d \end{bmatrix}^\dagger.$$

Then, the observer parameters are computed by $K_i = P^{-1}\Phi_i$ *and the relation is given in* Eqs. 17–18.

Proof The proof of Eq. 32 can be derived easily by considering the procedure described in [7]. □

Table 2 Incident matrix

Fault	F_0	F_1	F_2	...	F_p
$\| r^1 \|$	0	0	1	1	1
$\| r^2 \|$	0	1	1	1	1
...	0	1	1	0	1
$\| r^p \|$	0	1	1	1	0

Fig. 3 Pole placement

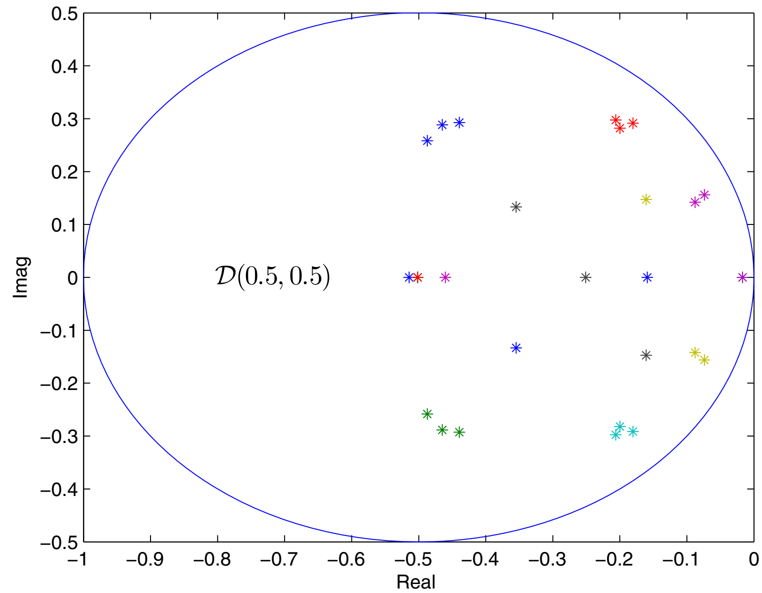

3.2 Sensor Fault Detection and Isolation

The purpose of this section is to use previous results to generate residuals to detect and isolate sensor faults. As pointed in [6], such that during fault-free operation, the magnitude of the residuals should be zero, or close to. In the presence of a fault, the residual should change its value, bigger than a predefined threshold, as an indication of fault occurrence. The residual generation is a process for extracting fault symptoms represented by the residual signals [6]. This step is necessary to avoid critical consequences and helps in taking appropriate decisions, either by shutting down the system safely, or continuing the operation in a degraded mode, despite the presence of the fault. To reach this objective, a Generalized Observer Scheme (GOS), as proposed in [9, 11], can be considered. This process is described as follows.

Under the presence of sensor faults, system Eq. 4 can be represented by

$$\dot{x}(t) = \sum_{i=1}^{h} \rho_i(x(t)) \left[A_i x(t) + B_i u(t) + R_i d(t)\right]$$
$$y(t) = Cx(t) + D_d d(t) + D_f f(t) \tag{33}$$

where $f(t)$ denotes the sensor fault vector. Clearly, from Fig. 2 it is easy to see that the fault diagnosis observer is decoupled from the controller, it means that the fault diagnosis observer can be designed separately. Then, by considering the GOS scheme, p observers are synthesized, where p is the number of sensor faults under consideration. A subsystem insensitive to a component f_p of the fault vector $f(t)$ is extracted for each observer by deriving the output vector $y(t)$. In order to isolate the sensor faults, a normalized residual vector is generated such that its p^{th} component is sensitive to all faults but p^{th} one. The bank of p fault diagnosis observers is given by

$$\dot{z}^p(t) = \sum_{i=1}^{h} \rho_i(x(t)) \left[N_i^p z(t) + G_i^p u(t) + L_i^p C^p x(t)\right]$$
$$\hat{x}^p(t) = z^p(t) + T_2 C^p x(t). \tag{34}$$
$$\| r^p(t) \| = \| W^p(y^p(t) - C^p \hat{x}^p(t)) \| . \tag{35}$$

Each observer satisfies observability condition. By solving the LMI system (21) for each set of given input matrices C^p the robustness and convergence are ensured. The bank of observers generates an incidence matrix as shown in Table 2. Each column is called the coherence vector associated to each fault signature.

It is clear from Table 2 that the decoupled observer method provides an efficient FDI technique for sensor faults. In the presence of a sensor fault, the observer, insensitive to the associated fault, estimates state vector $\hat{x}(t)$ and consequently estimates the output corrupted by the fault. Decision making can be carried-out according to an elementary binary logic.

3.3 Tracking Controller Design

By considering the comparator and integrator (8) and the system defined by Eq. 4, an augmented system $x_c(t) = [x^T(t) \quad \epsilon^T(t)]^T$ is obtained as:

$$\dot{x}_c(t) = \sum_{i=1}^{h} \rho_i(x(t) \left[\bar{A}_{ci} x_c(t) + \bar{B}_{ci} u(t) + \bar{R}_i d(t)\right] + \bar{B}_w w(t) \tag{36}$$

with

$$\bar{A}_{ci} = \begin{bmatrix} A_i & 0 \\ -C & 0 \end{bmatrix}, \ \bar{B}_c = \begin{bmatrix} B_i \\ 0 \end{bmatrix}, \ \bar{B}_w = \begin{bmatrix} 0 \\ I \end{bmatrix},$$
$$\bar{R}_i = \begin{bmatrix} R_i \\ -D_d \end{bmatrix}.$$

By assuming that pair $(\bar{A}_{ci}, \bar{B}_{ci})$ are controllable and by considering $u(t)$ as defined in Eq. 9, the following closed-loop system is obtained

$$\dot{x}_c(t) = \sum_{i=1}^{h} \rho_i(x(t) \sum_{j=1}^{h} \rho_j(x(t) \left[\left(\bar{A}_{ci} - \bar{B}_{ci}\mathcal{K}_j\right) x_c(t) + \bar{R}_i d(t)\right] + \bar{B}_w w(t) \tag{37}$$

Equivalently, Eq. 37 can be handled as:

$$\dot{x}_c(t) = \sum_{i=1}^{h} \rho_i(x(t) \sum_{j=1}^{h} \rho_j(x(t) \times \left[\left(\bar{A}_{ci} - \bar{B}_{ci}\mathcal{K}_j\right) x_c(t) + \bar{B}_{R\omega}\bar{d}_\omega(t)\right] \tag{38}$$

with

$$\bar{B}_{R\omega} = \left[\ \bar{R}_i \quad \bar{B}_\omega\ \right], \quad \bar{d}_\omega = \begin{bmatrix} d(t) \\ \omega(t) \end{bmatrix}$$

Sufficient conditions are given through the following Theorem to stabilize and control the system by considering the $\mathcal{L}_2$-gain from $\bar{d}_\omega(t)$ to $x_c(t)$.

Theorem 2 *Given system* (4)*, the comparator-integrator* (6)*, the feedback controller defined by* Eq. 9 *and let the attenuation level* $\gamma_c > 0$*. The closed loop system error* (38) *is globally stable with* H_∞ *performance if* $\| x_c(t)\|_2^2 < \gamma_c^2 \| \bar{d}_\omega(t)\|_2^2$ *and if there exists a matrix* $X = X^T \geq 0$ *such that* $\forall i, j \in [1, 2, ..., h]$*, the following holds:*

$$\begin{bmatrix} \mathrm{He}\left(X\bar{A}_{ci}^T + \Xi_j^T\bar{B}_{ci}^T\right) + \bar{B}_{R\omega}\bar{B}_{R\omega}^T & X \\ * & -\gamma_c^2 I \end{bmatrix} < 0. \tag{39}$$

Then, the controller gain matrices are computed by $\mathcal{K}_j = \left[\ K_{1j} \quad K_{2j}\ \right] = X_1^{-1}\Xi_j$*.*

Proof Similar to the observer design, the synthesis of the controller gains are done by considering the $\mathcal{L}_2$-gain from $\bar{d}_\omega(t)$ to $x_c(t)$ such that

$$J_{x_c d} := \dot{\Gamma}(t) + J_2 \tag{40}$$
$$J_2 = x_c^T(t)x_c(t) - \gamma_c^2\bar{d}_\omega(t)\bar{d}_\omega(t) < 0, \tag{41}$$

$J_{x_c d}$ represents the $\mathcal{L}_2$-gain of system (38) (from d to x_c) bounded by γ_c. $\Gamma(t)$ is a Lyapunov function defined as $\Gamma(t) = x_c^T(t)Px_c(t)(t)$. By considering the procedure described in the previous section, sufficient conditions are obtained as follows:

$$\begin{bmatrix} \left(\bar{A}_{ci} - \bar{B}_{ci}\mathcal{K}_j\right)^T P + P\left(\bar{A}_{ci} - \bar{B}_{ci}\mathcal{K}_j\right) + I & P\bar{B}_{R\omega} \\ * & -\gamma_c^2 I \end{bmatrix} < 0. \tag{42}$$

By considering $X = P^{-1}$ and pre- and post-multipliying Eq. 42 by $\begin{bmatrix} X & 0 \\ 0 & I \end{bmatrix}$, the following LMI is rewritten as:

$$\begin{bmatrix} X\bar{A}_{ci}^T + \bar{A}_{ci}X + X^T X & \bar{B}_{R\omega} \\ * & -\gamma^2 I \end{bmatrix} < 0,$$

Finally by considering the Schur complement of $X^T X$ and $\bar{B}_{R\omega}$ the LMI (39) is derived. This complete the proof. □

Remark 1 The minimization of γ_c may result in slow dynamics of the state estimation error. This problem can be solved by pole assignment of the matrices $(\bar{A}_{ci} - \bar{B}_{ci}\mathcal{K}_j)$ in left half complex plane such that

$$\lambda_j(\bar{A}_{ci} - \bar{B}_{ci}\mathcal{K}_j) \in \mathbb{D}, \ j = 1, 2, ..., n; \ i = 1, 2, ..., h,$$

$\mathbb{D}$ is the α stability region as defined in [8]. Then the following Corollary is obtained.

Corollary 2 *Given system* (4)*, the comparator-integrator* (6)*, the feedback controller defined by* Eq. 9 *and let the attenuation level* $\gamma_c > 0$*. The closed-loop system error* Eq. 38 *is globally stable with* H_∞ *performance if* $\| x_c(t)\|_2^2 < \gamma_c^2 \| d(t)\|_2^2$ *and if there exist a matrix* $X = X^T \geq 0$*, and a positive scalar* α *such that* $\forall i, j \in [1, 2, ..., h]$*, the following holds:*

$$\begin{bmatrix} Z_i + \bar{B}_{R\omega}\bar{B}_{R\omega}^T + 2\alpha P & X \\ * & -\gamma_c^2 I \end{bmatrix} < 0 \quad (43)$$

with

$$Z_i = X\bar{A}_{ci}^T + \bar{A}_{ci}X + \Xi_j^T\bar{B}_{ci}^T + \bar{B}_{ci}\Xi_j.$$

Then, the controller gain matrices are computed by $\mathcal{K}_j = \begin{bmatrix} K_{1j} & K_{2j} \end{bmatrix} = X_1^{-1}\Xi_j$.

Proof The proof is easily derived by considering the α-stability in the $\mathscr{L}_2$-gain equation (22), such that

$$J_{x_c d} := \dot{\Gamma} + J_2 + 2\alpha\Omega < 0. \quad (44)$$

By solving Eq. 44, the conditions described in the LMI are derived. □

Remark 2 The LMI set (43) can bring conservatism into the observer design due to the LMI dimension, the number of models, and the requirement of a single matrix P and Q. Then, without loss of good compromise between complexity and conservatism, the following LMIs set can be considered (see details in [4]):

$$\Upsilon_{ii} < 0 \quad (45)$$

$$\frac{2}{h-1}\Upsilon_{ii} + \Upsilon_{ij} + \Upsilon_{ji} < 0 \quad (46)$$

where Υ_{ij} is given by Eq. 43.

4 Simulation Results

The proposed design approach applied to the quadrotor is illustrated on this section. The matrices of Eq. 4 are not displayed here due to space limitations, however these can be consulted in the referenced paper [12]. For simulation purpose, additional disturbance matrices are considered as:

$$R_i = [1, 0, ..., 0]^T, \quad D_d = \begin{bmatrix} 0.2 \\ 0.4 \\ 0.5 \\ 0.3 \end{bmatrix},$$

and in order to achieve the nonlinear dynamic, convex scheduling functions are defined as:

$$\rho_i(x(t)) = \frac{\mu_i(x(t))}{\sum_{i=1}^{3}\mu_i(x(t))}$$

$$\mu_1(x(t)) = exp\left[\frac{1}{2}\left(\frac{x_4(t)+1.8}{0.8}\right)^2\right]$$

$$\mu_2(x(t)) = exp\left[\frac{1}{2}\left(\frac{x_4(t)-1.8}{0.8}\right)^2\right]$$

$$\mu_3(x(t)) = exp\left[\frac{1}{2}\left(\frac{x_4(t)}{0.8}\right)^2\right]. \quad (47)$$

The synthesis of the stable LPV observer with H_∞ performance (6) has been solved with Yalmip Toolbox [15]. The attenuation level obtained by solving Corollary 1. The observer eigenvalues are assignment in a disk $\mathcal{D}(0.5, 0.5)$ with center $(-0.5, 0)$ and radius 0.5. The computed attenuation level is $\gamma = 0.4965$. The computed parameter matrices are:

$$P = \begin{bmatrix}
0.39 & -0.009 & 0 & 0 & -0.0031 & -0.000 & -0.05 & 0.0009 & 0 & 0 & 0.002 & 0 \\
-0.009 & 0.84 & 0 & 0 & 0.0049 & 0.027 & 0.004 & -0.1785 & 0 & 0.0049 & -0.004 & 0 \\
0 & 0 & 2.48 & 0.0001 & 0 & -0.00 & 0 & 0 & -0.061 & 0.0001 & 0 & -0.0 \\
0 & 0 & 0.001 & 2.49 & 0.0002 & 0.002 & 0 & 0 & 0.0001 & -0.0001 & -0.0003 & -0.06 \\
-0.003 & 0.005 & 0 & 0.0002 & 5.62 & -0.007 & 0.04 & -0.006 & 0 & -0.006 & 0.46 & 0 \\
-0.002 & 0.028 & -0.0004 & 0.0002 & -0.007 & 6.2508 & 0 & -0.23 & 0.002 & 0.079 & -0.014 & 0 \\
-0.056 & 0.04 & 0 & 0 & 0.04 & 0 & 0.174 & -0.0002 & 0 & 0 & -0.0005 & 0 \\
0.0009 & -0.17 & 0 & 0 & -0.0058 & -0.22 & -0.0002 & 0.23 & 0 & -0.0137 & 0.0005 & 0 \\
0 & 0 & -0.061 & 0.0001 & 0 & 0.002 & 0 & 0 & 2.3891 & -0.0006 & 0 & -0. \\
0 & 0.004 & 0.001 & -0.0001 & -0.00 & 0.079 & 0 & -0.0137 & -0.0006 & 3.45 & -0.004 & 0.004 \\
0.002 & -0.004 & 0 & -0.0003 & 0.46 & -0.014 & -0.0005 & 0.0005 & 0 & -0.004 & 3.4 & 0.002 \\
0 & 0 & -0.001 & -0.0615 & 0 & 0.002 & 0 & 0 & -0.0003 & 0.0004 & 0.0002 & 2.3
\end{bmatrix}$$

$$\Phi_3 = \begin{bmatrix} 1.3492 & -0.3713 & -0.0004 & -0.0002 \\ -0.2873 & 1.0983 & -0.0004 & -0.0003 \\ -0.0001 & 0 & 1.2812 & 0.0001 \\ -0.0005 & 0.0006 & 0.0002 & 1.2822 \\ 0.0542 & -0.0042 & 0.0035 & -0.0008 \\ 0.0368 & -0.0472 & -0.0046 & -0.0084 \\ -0.0401 & 0.0064 & 0.0004 & 0.0002 \\ -0.0311 & -0.0659 & 0.0003 & 0.0007 \\ 0 & 0.0001 & 0.0082 & 0.0003 \\ 0.0047 & -0.0003 & 0.0042 & 0 \\ 0.0051 & -0.0055 & 0 & -0.0007 \\ 0.0009 & -0.0006 & -0.001 & 0.009 \end{bmatrix}$$

The observer gain matrices are computed by $K_i = P^{-1}\Phi_i$ and the relation given in Eqs. 17–18. Matrices T_1 and T_2 are not displayed here due to space limitation, but can be computed from Eq. 20. Furthermore, as displayed in Fig. 3, the observer eigenvalues of N_i are located in the selected LMI region.

The controller gains are computed by solving the Corollary 2. A LMI region with $\alpha = 1.5$ was chosen to avoid slow dynamics. The computed attenuation level is $\gamma_c = 0.4501$, which is small and can guarantee the desired performance. The controller gains are:

$$\mathcal{K}_{x1} = \begin{bmatrix} 0 & 0 & 7.24 & 0 & 0 & 0 & 0 & 0 & 3.6 & 0 & 0 & 0 & 0 & 0 & -3.93 & 0 \\ 14.6 & -229 & 0 & 0 & -38 & -741 & 11.9 & -185.4 & 0 & -92.9 & -4.6 & 0 & -6.6 & 101 & 0 & 0 \\ 221.7 & 12.3 & 0 & 0 & -737.5 & 36.5 & 180 & 10 & 0 & 4 & -93 & 0 & -98 & -5.14 & 0 & 0 \\ 0 & 0 & 0 & -12.842 & 0 & 0 & 0 & 0 & 0 & 0 & 0 & -6.387 & 0 & 0 & 0 & 6.9 \end{bmatrix}$$

$$\mathcal{K}_{x2} = \begin{bmatrix} 0 & 0 & 7.24 & 0 & 0 & 0 & 0 & 0 & 3.60 & 0 & 0 & 0 & 0 & 0 & -3.93 & 0 \\ 1.18 & -226 & 0 & 0 & -1.21 & -729 & 0.80 & -18 & 0 & -91 & -0.042 & 0 & -0.36 & 100 & 0 & 0 \\ 219 & -1.69 & 0 & 0 & -726 & -1.47 & 178 & -0.86 & 0 & -0.037 & -91 & 0 & -97 & 1.38 & 0 & 0 \\ 0 & 0 & 0 & -12.8 & 0 & 0 & 0 & 0 & 0 & 0 & 0 & -6.38 & 0 & 0 & 0 & 6.9 \end{bmatrix}$$

$$\mathcal{K}_{x3} = \begin{bmatrix} 0 & 0 & 7.24 & 0 & 0 & 0 & 0 & 0 & 3.6 & 0 & 0 & 0 & 0 & 0 & -3.93 & 0 \\ -12.19 & -229 & 0 & 0 & 35 & -741 & -10.33 & -185 & 0 & -92 & 4.60 & 0 & 5.91 & 101 & 0 & 0 \\ 222 & -15.8 & 0 & 0 & -737 & -39.5 & 180 & -12.4 & 0 & -4.77 & -93.01 & 0 & -98 & 7.95 & 0 & 0 \\ 0 & 0 & 0 & -12.8 & 0 & 0 & 0 & 0 & 0 & 0 & 0 & -6.38 & 0 & 0 & 0 & 7 \end{bmatrix}$$

For simulation purpose, the perturbation $d(t)$ is chosen as random signal uniformly distributed in $[-0.5, 0.5]$. Initial conditions are considered as $x(0) = [0.2,\ 0.5,\ 0,\ 1.2217,\ 0,\ ...,\ 0]^T$ and $\hat{x}(0) = [0.2,\ 0.3,\ 0,\ ...,\ 0]^T$. In practice, initial conditions are chosen according to the initial measured value

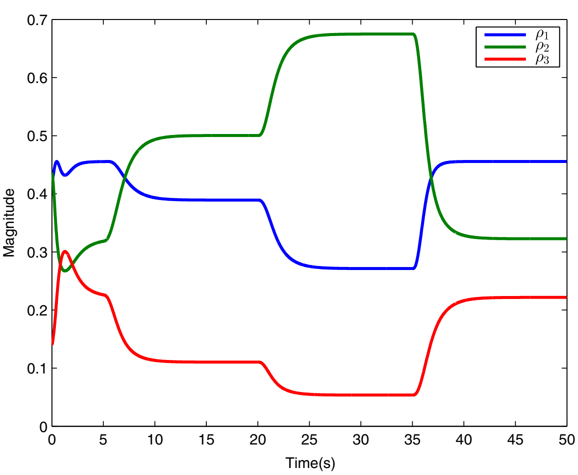

Fig. 4 Gain scheduling functions

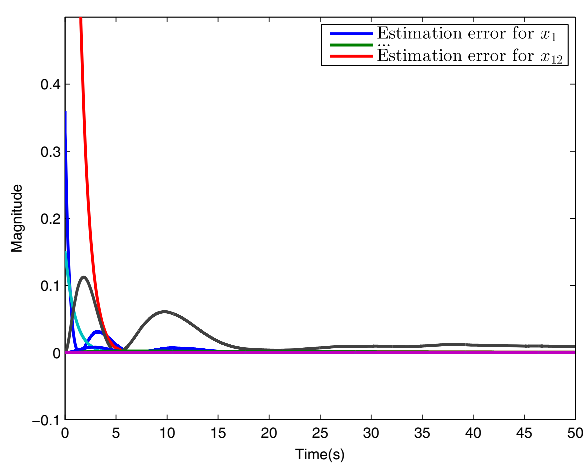

Fig. 5 State estimation errors

of the positions. Actuator saturation is not taking into consideration. Simulation results are displayed as follows. Figure 4 shows the contribution of each model to the global behavior, as defined by the scheduling functions.

Figure 5 displays the estimation errors between the estimated and the simulated states. As displayed, the observer converges fast and asymptotically. Moreover, the disturbances are well attenuated, which validates the observer performance.

Figure 6 shows the references and tracking trajectory of the positions (x, y, z) and the yaw angle ψ in fault-free operation. The tracking is well performed, despite the disturbance and the set-up variations on the reference.

In order to prove the effectiveness of the proposed method under faults, a bank of 4 residual generators (one for each output) are designed, as described in Section 3.2. Two sensor faults are induced as displayed in Fig. 7e. The first fault, occurring on the second sensor, after $t = 45$ s, is a fault with bias behavior. The second fault, which appears from $t =$ 12 s to 26 s, is a fault with sinusoidal behavior on thethird sensor. The normalized residual signals are displayed in Fig. 7a–d. The fault detection can be done easily by comparing the residuals with the incidence matrix given in Table 2. For example, for the second fault occurred on the sensor 3, residuals r_1, r_2 and r_4 present some changes at $t = 12$ s, and only residual r_3 remains without change. So, it is possible to generate a particular signature $S = [1 \ \ 1 \ \ 0 \ \ 1]$. Then, by comparing the signature with Table 2, it is possible to isolate the fault on sensor 3. Clearly, for all cases, the fault detection turns out to be successful.

The tracking positions are displayed in Fig. 8. When the first fault appears at $t = 45$ s, the position y is affected, but due to the fact that the controller was designed with H_∞ performance, after three seconds the quadrotor reaches again the desired position. This behavior is not reflected with respect to the second

Fig. 6 Desired position (*dashed line*) and real positions (*continuous line*)

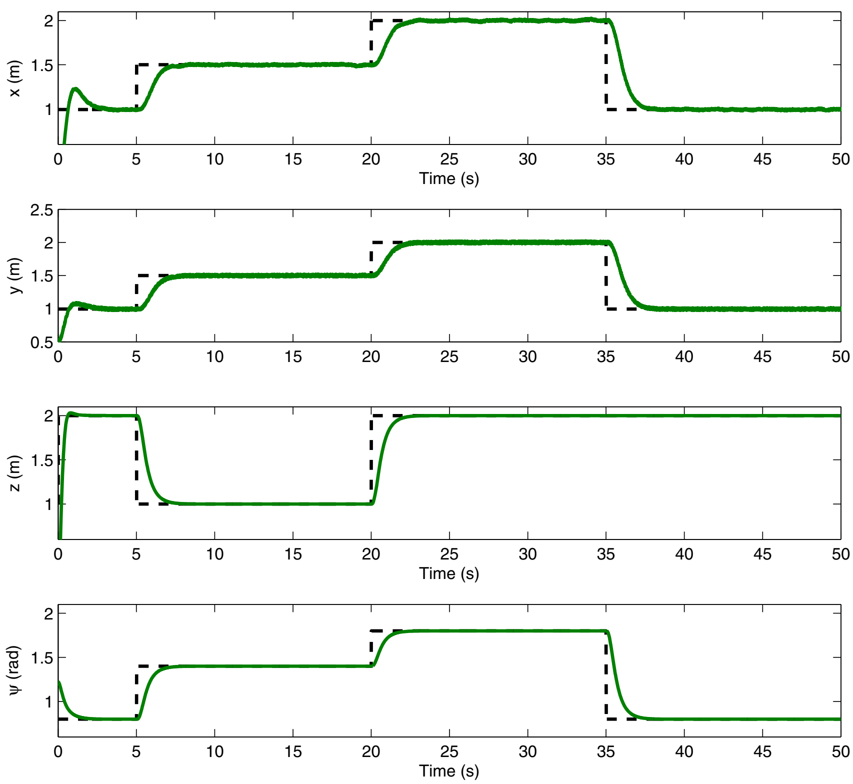

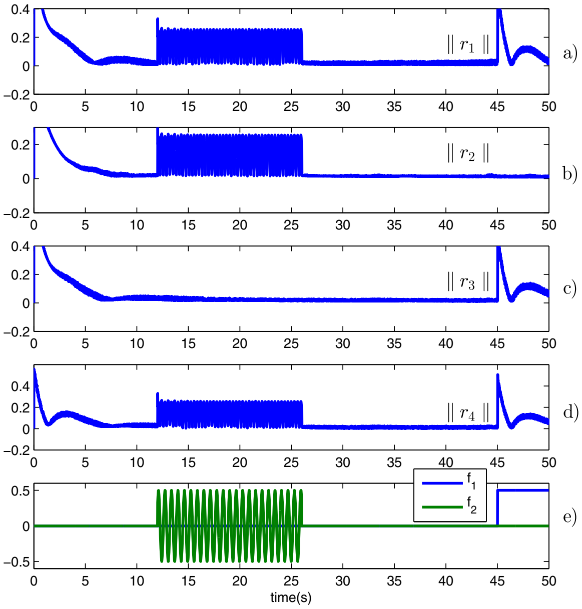

Fig. 7 **a–d** Normalized residuals in faulty-case; **e** induced faults

fault, due that the fault is continuously changing fast, because of the sinusoidal behavior. However, once that fault disappears, the output converges again to the desired position. In order to guarantee tracking for all outputs in the presence of faults, a fault tolerant control strategy will be addressed in future work.

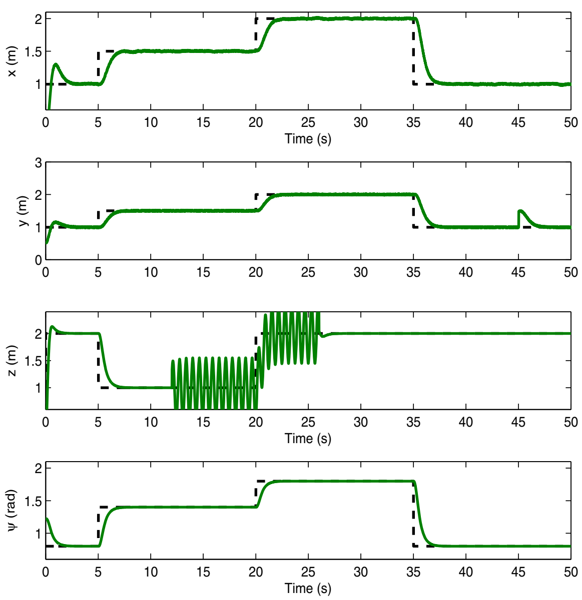

Fig. 8 Desired position (*dashed line*) and real positions (*continuous line*) in faulty-case

5 Conclusions

In this paper, a tracking controller and robust fault diagnosis was developed for LPV systems in the presence of disturbances. Using Lyapunov and $\mathscr{L}_2$-gain theory, sufficient conditions in the LMI formulation were obtained. In the same spirit, sufficient conditions were obtained to compute the gains of the controller in order to stabilize the nonlinear system and track the command signal. In order to detect and isolate sensor faults, a set of residuals was generated with a bank of observers so that each residual is sensitive to only one fault. Each observer was designed to be robust against disturbances. Then, using a LPV modelisation of a quadrotor, the developed methodology is applied to this type of UAV. The simulation results have shown the effectiveness of the proposed methodology. Future research will be addressed on the topic of fault tolerant control.

Acknowledgments This work was supported by CONACyT (Consejo Nacional de Ciencia y Tecnología), Mexico, and the Ministère des Affaires Étrangères, France. The supports are gratefully acknowledged. Moreover, the authors would like to thank Professor Francisco Jurado (Instituto Tecnológico de la Laguna, Mexico) for his advice and help with the nonlinear model. Finally thank to the reviewers for their useful comments.

References

1. Asemani, M.H., Majd, V.J.: A robust H_∞ observer-based controller design for uncertain T-S fuzzy systems with unknown premise variables via LMI. Fuzzy Sets Syst. **212**, 21–40 (2012)
2. Briat, C.: Linear Parameter-Varying and Time-Delay Systems - Analysis, Observation, Filtering & Control, Volume 3 of Advances on Delays and Dynamics. Springer-Verlag, Heidelberg (2014)
3. Cen, Z., Noura, H., Susilo, T.B., Al Younes, Y.: Robust fault diagnosis for quadrotor UAVs using adaptive thau observer. J. Intell. Robot. Syst. **73**(1–4), 573–588 (2014)

4. Chadli, M., Abdo, A., Ding, S.X.: Fault detection filter for discrete-time Takagi-Sugeno fuzzy system. Automatica **49**(7), 1996–2005 (2013)
5. Chadli, M., Karimi, H.R.: Robust observer design for unknown inputs Takagi-Sugeno. IEEE Trans. Fuzzy Syst. **21**(1), 158–164 (2013)
6. Chen, J., Patton, R.J.: Robust Model-Fault Diagnosis for Dynamic Systems. Springer, US (1999)
7. Chilali, M., Gahinet, P., Apkarian, P., Member, A.: Robust pole placement in LMI regions. IEEE Trans. Autom. Control **44**(12), 2257–2270 (1999)
8. Duan, G.R., Yu, H.H.: LMIs in Control Systems. CRC Press, Taylor and Francis (2013)
9. Frank, P.: Fault diagnosis in dynamic systems using analytical and knownledge-based redundancy: a survey and some new results. Automatica **26**(3), 459–474 (1990)
10. Guang-Xun, D., Quan, Q., Cai, K.Y.: Controllability analysis and degraded control for a class of hexacopters subject to rotor failures. J. Intell. Robot. Syst. **78**(1), 143–157 (2015)
11. Isermann, R.: Fault-Diagnosis Systems: An Introduction from Fault Detection to Fault Tolerance. Springer-Verlag, Berlin Heidelberg (2006)
12. Jurado, F., Castillo-Toledo, B., Di-Gennaro, S.: Stabilization of a quadrotor via takagi-sugeno fuzzy control. In: 12th World Multi-Conference on Systemics, Cybernetics and Informatics (WMSCI). Orlando (2008)
13. Lendek, Z., Berna, A., Guzman-Gimenez, J., Sala, A., Garcia, P.: Application of takagi-sugeno observers for state estimation in a quadrotor. In: 50th IEEE Conference on Decision and Control and European Control Conference (CDC-ECC). Orlando (2011)
14. Lim, H., Park, J., Lee, D., Kim, H.J.: Build your own quadrotor: Open-source projects on unmanned aerial vehicles. IEEE Robot. Autom. Mag. **19**(3), 33–45 (2012)
15. Lofberg, J.: A toolbox for modeling and optimization in MATLAB. In: Proceedings of the Computer Aided Control System Design Conference. Taipei (2004)
16. López-Estrada, F., Ponsart, J., Theilliol, D., Astorga-Zaragoza, C.: Robust H_{-/H_∞} fault detection observer design for descriptor-LPV systems with unmeasurable gain scheduling functions. Int. J. Control (In-press) (2015). doi:10.1080/00207179.2015.1044261
17. López-Estrada, F.R., Ponsart, J.C., Astorga-Zaragoza, C.M., Camas-Anzueto, J.L., Theilliol, D.: Robust sensor fault estimation for descriptor–LPV systems with unmeasurable gain scheduling functions: Application to an anaerobic bioreactor. Int. J. Appl. Math. Comput. Sci. **25**(2), 233–244 (2015)
18. López-Estrada, F.R., Ponsart, J.C., Theilliol, D., Astorga-Zaragoza, C., Zhang, Y.: Robust sensor fault diagnosis and tracking controller for a uav modelled as lpv system. In: International Conference on Unmanned Aircraft Systems. Orlando, Florida (2014)
19. Mistler, V., Benallegue, A., M'Sirdi, N.: Exact linearization and noninteracting control of a 4 rotors helicopter via dynamic feedback. In: 10th IEEE InternationalWorkshop on Robot and Human Interactive Communication, pp. 586–593 (2001)
20. Office of the Secretary of Defense: Unmanned aerial vehicles roadmap 2002–2027. Tech. rep. Washington, DC (2002)
21. Qi, X., Qi, J.T., Theilliol, D., Zhang, Y.M., Han, J.D., Song, D.L., Hua, C.: A review on fault diagnosis and fault tolerant control methods for single-rotor aerial vehicles. J. Intell. Robot. Syst. **73**(1–4), 535–555 (2014)
22. Raffo, G.V., Ortega, M.G., Rubio, F.R.: An integral predictive/nonlinear H_∞ control structure for a quadrotor helicopter. Automatica **46**(1), 29–39 (2010)
23. Rodrigues, M., Hamdi, H., BenHadj-Braiek, N., Theilliol, D.: Observer-based fault tolerant control design for a class of LPV descriptor systems. J. Frankl. Inst. **351**(6), 3104–3125 (2014)
24. Rotondo, D., Nejjari, F., Puig, V.: Robust quasi-LPV model reference FTC of a quadrotor UAV subject to actuator faults. Int. J. Appl. Math. Comput. Sci. **25**(1), 7–22 (2015)
25. Samy, I., Postlethwaite, I., Gu, D.W.: Survey and application of sensor fault detection and isolation schemes. Control. Eng. Pract. **19**(7), 658–674 (2011)
26. Saul, M.D.O., Puig, V., Witczak, M., Quevedo, J.: Fault-tolerant control of a two-degree of freedom helicopter using LPV techniques. In: 16th Mediterranean Conference on Control and Automation, pp. 1204–1209 (2008)
27. Serirojanakul, A., Wongsaisuwan, M.: Optimal control of quad-rotor helicopter using state feedback LPV method. In: 9th International Conference on Electrical Engineering/Electronics, Computer, Telecommunications and Information Technology (ECTI-CON). Hua Hin, Thailand (2012)
28. Shamma, J.: An overview of LPV systems. In: Mohammadpour, J., Scherer, C.W. (eds.) Control of Linear Parameter Varying Systems with Applications, pp. 3–26. Springer, US (2012)
29. Takagi, T., Sugeno, M.: Fuzzy identification of systems and its applications to modeling and control. IEEE Trans Syst Man Cybern **SMC-15**(1), 116–132 (1985)
30. Theilliol, D., Aberkane, S.: Desing of LPV observers with unmeasurable gain scheduling variable under sensors faults. In: IFAC World Congress. Milano, Italy (2011)
31. Vermeiren, L., Dequidt, A., Afroun, M., Guerra, T.M.: Motion control of planar parallel robot using the fuzzy descriptor system approach. ISA Trans. **51**(5), 596–608 (2012)
32. Zhang, Y.M., Chamseddine, A., Rabbath, C., Gordon, B., Su, C.Y., Rakheja, S., Fulford, C., Apkarian, J., Gosselin, P.: Development of advanced FDD and FTC techniques with application to an unmanned quadrotor helicopter testbed. J. Frankl. Inst. **350**(9), 2396–2422 (2013)
33. Zhang, Y.M., Jiang, J.: Bibliographical review on reconfigurable fault-tolerant control systems. Annu. Rev. Control. **32**, 229–252 (2008)

Francisco Ronay López-Estrada was a Ph.D.student at the Research Centre for Automatic Control of Nancy, France and received hid Ph.D. in 2014 from the University of Lorraine. He is now an Associated Professor in the Insituto Tecnológico de Tuxtla Gutiérrez, Mexico. He received his M.Sc.degree in Electronic Engineering in Feb.2008 from the Centro Nacional de Investigación y Desarrollo Tecnológico (CENIDET), Mexico. His research interests are in descriptor systems, linear parameter varying systems, fault detection and fault tolerant control systems and applications to UAV.

Jean-Christophe Ponsart received his Ph.D. in 1996 from the University of Savoie in Annecy, France, in nonlinear control of magnetic suspensions and its digital implementation aspects. In 1997, he participated in design and implementation of real time controllers with digital signal processor architecture for an industrial company. He has been with the Research Center for Automatic Control of Nancy (CRAN) at the University of Lorraine since 1998 as an Assistant Professor. In 2011, he obtained the *Habilitation à Diriger des Recherches* (HDR) from the University of Lorraine. His current interests include fault diagnosis and accommodation, and fault-tolerant control applied to LPV and nonlinear systems. Currently, he develops these topics on UAV applications among others.

Didier Theilliol received the Ph.D. degree in Control Engineering from University of Lorraine (France) in 1993. Since September 2004, he is a full Professor in Research Centre for Automatic Control of Nancy (CRAN) at University of Lorraine where he co-ordinates and leads national, European and International R&D projects in steel industries, wastewater treatment plant and aerospace domains. His current research interests include sensor and actuator model-based fault diagnosis (FDI) method synthesis and active fault-tolerant control (FTC) system design for LTI, LPV, Multi-linear systems and also reliability analysis of components. Prof. Theilliol published over 200 journal/conference papers and is a co-author of a book entitled 'Fault-tolerant Control Systems: Design and Practical Applications' (2009). He was during two years Visiting Professorship for Senior International Scientists for Chinese Academy of Sciences. He is one of European Advanced Control and Diagnosis (EACD) steering committee members and is also a member of IFAC Technical Committee 6.2. Mining, Mineral and Metal Processing. He is currently an Associate Editor of IEEE Transactions on Reliability, ISA Transactions Journal, Unmanned Systems journal, International Journal of Applied Mathematics & Computer Science and more recently Journal of Intelligent and Robotic Systems.

Youmin Zhang received the B.S., M.S., and Ph.D. degrees with a specialization in automatic controls from Northwestern Polytechnical University, Xi'an, China, in 1983, 1986, and 1995, respectively.

Dr. Zhang is currently a Professor with the Department of Mechanical and Industrial Engineering and the Concordia Institute of Aerospace Design and Innovation, Faculty of Engineering and Computer Science, Concordia University, Montreal, Quebec, Canada. His current research interests include condition monitoring, health management, fault diagnosis, and fault-tolerant (flight) control systems, cooperative guidance, navigation, and control of unmanned aerial/space/ground/surface vehicles, dynamic systems modeling, estimation, identification, advanced control techniques and advanced signal processing techniques for diagnosis, prognosis, and health management of safety-critical systems, renewable energy systems and smart grids, and manufacturing processes. He has authored four books, over 380 journal and conference papers, and book chapters.

Prof. Zhang is a Senior Member of the American Institute of Aeronautics and Astronautics (AIAA) and the Institute of Electrical and Electronics Engineers (IEEE), and a member of the Technical Committee (TC) for several scientific societies, including the International Federation of Automatic Control (IFAC) TC on Fault Detection, Supervision and Safety for Technical Processes (SAFEPROCESS), Chinese SAFEPROCESS, the AIAA Infotech@Aerospace Program Committee on Unmanned Systems, the IEEE Robotics and Automation Society TC on Aerial Robotics and Unmanned Aerial Vehicles, the ASME/IEEE TC on Mechatronics and Embedded Systems and Applications, and the International Conference on Unmanned Aircraft Systems (ICUAS) Association Executive Committee. He has been invited to deliver plenary talks at international conferences/workshops and research seminars worldwide for over 50 times. He is the Editor-in-Chief of the Journal of Instrumentation, Automation and Systems, an Editorial Board Member, and/or Editor-at-Large, Senior or Associate Editor of six other international journals (including three newly launched journals on Unmanned Systems). He has served as the General Chair, the Program Chair, the Program Vice Chair, and IPC Member of many international conferences, including the General Chair of the 10th International Conference on Intelligent Unmanned Systems (ICIUS) in 2014, Montreal, Canada, the Program Chair of the International Conference on Unmanned Aircraft Systems (ICUAS) in 2014, Orlando, FL, USA, and one of General Chairs of the ICUAS in 2015, Denver, CO, USA.

Carlos-Manuel Astorga-Zaragoza was born in Minatitlán, Veracruz, Mexico, in 1967. He received the M.Sc. degree in electronic engineering from the Centro Nacional de Investigación y Desarrollo Tecnológico (CENIDET), Cuernavaca, Morelos, Mexico, in 1993, and the Ph.D. in process engineering from the Université Claude Bernard Lyon 1, France, in 2001. Since 1993, he has held teaching and research positions at the CENIDET, where he mainly works on automatic control of energy conversion processes. His research interests include thenonlinear observers, fault diagnosis, and control systems with applications. In 2009 he performed a postdoctoral stage at Centre de Recherche en Automatique de Nancy, France. He was Editor of the 8th IFAC Symposium on Fault Detection, Supervision and Safety for Technical Processes, SAFEPROCESS 2012 and the General Chair of the National Congress of Automatic Control, AMCA 2015, in Mexico.